Triple-GEM detectors for electron, proton and neutron beam diagnostics

Paolo Valente[a], Giovanni Corradi[b], Fabrizio Murtas[b], Marco Pistilli[b], Diego Tagnani[b], Basilio Esposito[c], Daniele Marocco[c]

[a] *INFN Sezione di Roma, Roma, Italy*
[b] *Laboratori Nazionali di Frascati dellINFN, Frascati, Italy*
[c] *ENEA, Frascati, Italy*

Abstract

Different detectors based on triple GEM technology, realized in Frascati during the last years, are presented. They have been used for the luminosity measurements at the DAFNE Φ-Factory; for the beam position monitor at the BTF beam-test facility in Frascati, for the UA9 experiment at the CERN H8 beam-line, and in the SPS circulating beam; and for the high-intensity neutron flux measurements at FNG and Frascati Tokamak Upgrade. We also report on the design, construction and test of a GEM compact time projection chamber (TPC), for beam tracking. A description of the detector construction and assembly, together with the results achieved during tests at BTF and CERN, is also given.

Key words: Micro-pattern gas detectors, GEM, neutron monitor, beam monitor, TPC
PACS: 29.40.Cs, 29.40.Gx

1. Introduction

A GEM (gas electron multiplier) is made of a thin (50 μm) kapton foil, a copper cladding on each side, perforated with a high surface density of holes, each one acting as an electron multiplication channel. Each hole has a bi-conical structure with external (internal) diameter of 70 μm (50 μm) and a pitch of 140 μm [1]. The bi-conical shape of the hole minimises the effect of charging-up of the kapton inside the holes (with respect to the conical shape) and is a consequence of the double mask process used in standard photolitographic technologies.

When applying a voltage difference of 350 to 500 V between the two copper sides, an electric field as high as 100 kV/cm is created into the holes, resulting in an electron multiplication of up to a few thousands. Multiple structures realized by assembling two or more GEMs at close distance allow high gains to be reached while minimising the discharge probability.

In the last years, several triple-GEM detectors have been realized: they consist of three GEM foils sandwiched between two conductive planes, one of them, the anode, is segmented in pads and connected to the readout electronics, in order to collect the charge induced by the drifting electron cloud originating from the last GEM stage; in this way the gas amplification and the signal readout are completely separated [2].

All detectors we report on here are built starting from the standard 10×10 cm^2 active area GEM foils produced by CERN. The GEMs are stretched and a G10 frame, 12×12 cm^2, is glued on top; the three frames are successively glued together forming four gaps (3, 1, 2, 1 mm). The anode PCB, 12×12 cm^2, has been designed with the idea of housing 128 pads of different geometries inside the active area, while keeping eight connectors for the front-end electronics (FEE) on the opposite side.

The FEE boards used for this development are based on the Carioca-GEM chip [3]; each board houses 16 ASD channels (two chips) producing LVDS time over threshold signals. The small dimensions of these boards (3×6 cm^2) allow the assembling of eight cards within the detector dimension, while a mother board is plugged just on top of the eight boards for low voltage power supply and threshold distribution, as well as for high voltage filters.

The LV supply of 2.5 V and the threshold settings are driven through a NIM module that can be set manually or remotely, through a VME programmable DAC.

The chambers are flushed with a gas mixture Ar/CO_2 (70%/30%). The HV power is provided through the HVGEM module [4]: starting from the 12 V supply voltage this device creates the three GEM voltages determining the chamber gain, and the four voltages producing the electric fields for the electron cascade drift.

2. UA9 experiment at the SPS

The UA9 experiment intends to assess the possibility of using bent silicon crystals as primary collimators to direct coherently the beam halo onto the secondary absorber, thus reducing out-scattering, beam losses in critical regions, and radiation load [5]. The experiment is performed in the CERN-SPS in storage mode with a 120 or 270 GeV/c proton beam, and the otherwise stable beam is perturbed to create a diffusive halo. The setup consists of several stations tracking the halo particles before and after the crystal goniometer vacuum station.

We have installed two dedicated triple-GEMs (10×10 cm^2, 8×16 pads of size 12×6 mm^2) at large angle with respect to the expected main particle trajectories. The two detectors have been placed upstream and downstream of the crystal station, just outside the SPS beam pipe, with the aim of tracking

off-momentum beam losses induced by the collimation process and particles randomly scattered in the (amorphous) interaction with the crystal. As a main result, we were able to detect the channeling condition looking at the total rate on the GEM pads, due to the reduced number of particles in the beam halo. In Fig. 1 the rate of the GEM pads as a function of the angle of the bent-crystal with respect to the incoming SPS beam, showing the main and the secondary channeling peaks (dips in the scattered particles rate).

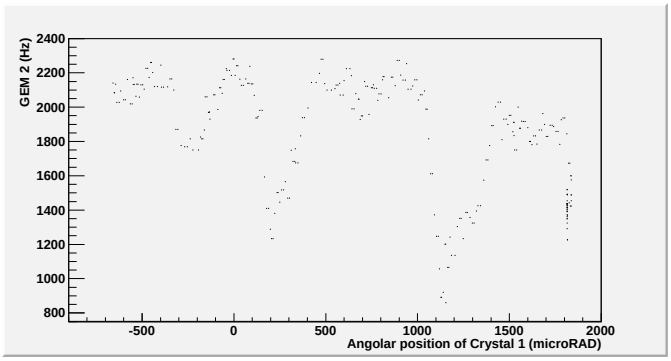

Figure 1: Rate on the triple-GEM detector downstream of the vacuum tank holding the UA9 experiment goniometer/bent crystal setup, as a function of the angle with respect to the SPS beam during an angular scan. The several channeling peaks (dips in the counting rate) are clearly visible.

3. Neutron beam monitor

In controlled thermonuclear fusion devices the fusion power is assessed through the measurement of the neutrons emitted from the plasma. The two reactions employed in fusion experiments (DD and DT) yield 2.5 MeV and 14 MeV neutrons respectively. These two neutron components must be measured separately in future fusion reactors. In order to obtain a fast neutron detector, we have coupled a triple-GEM to a proton-recoil converter (polyethylene) and to an absorber (aluminum). The recoil protons, generated by (n,p)-reactions in polyethylene and having enough energy to cross the aluminum foil, lose their energy by ionization of the gas atoms. The generated electrons are amplified in the GEM layer structure giving a detectable signal. The thickness of the polyethylene and aluminum foils can be optimized in order to set a threshold lower than the energy of neutrons from DT (14 MeV), or from DD reactions (2.5 MeV) [6].

In order to optimize this kind of neutron detectors, we have realized a triple-GEM detector with both the proton-recoil converter and absorber foils segmented in two halves with different thickness: 2 mm of polyethylene and 0.2 mm of aluminum for the DT half, and 700 μm of polyethylene and 5 μm of aluminum for the DD half. This detector has been tested at the ENEA Frascati Neutron Generator facility (FNG), capable of producing 14 MeV or 2.5 MeV neutrons with fluxes of up to 10^{11} n/s in steady state or pulsed mode. The detector installed at the FNG neutron facility is shown in Fig. 2.

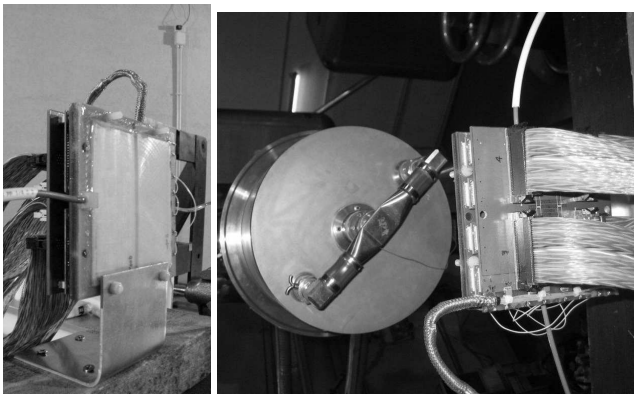

Figure 2: Triple-GEM neutron monitor: on the left, the two halves with different polyethylene and aluminum adsorber thickness on the cathode are clearly visible; on the right, the detector with the read-out, HV and gas connections, mounted in front of the neutron FNG beam source in Frascati (at ≈ 0.5 m distance).

The response of the two halves can be easily compared, both online and offline, by looking at the corresponding 12×6 mm^2 pads (4×16 each).

We have performed measurements of the efficiency by comparing the DT/DD pads rate with the neutron flux (that can be adjusted by the user and is monitored by means of NE-213 scintillator counters) as a function of the threshold and of the total gain of the triple-GEM, with the aim of finding the optimal working-point for the DT and DD neutron monitor and of keeping, at the same time, a very low efficiency to photons. In order to check the response of the detector to $\sim$ MeV photons, we also measured the efficiency using ^{60}Co (1.2 MeV) and ^{137}Cs (0.7 MeV) γ-sources. The overall results are shown in Fig. 3. Once having set a relatively high threshold, $\sim$ 6 fC, for the Carioca-GEM electronics, it is possible to find a region in the gain-scan such that, at the same time, the detection efficiency for 2.5 MeV neutrons of the DD detector is higher (up to one order of magnitude) than that of the DT detector, and both detector halves are well over threshold for 14 MeV neutrons (with comparable efficiencies). Moreover, in this gain region both detectors are practically blind to photons.

4. Compact Time-Projection GEM (TPG)

The main motivation for this detector comes from the need of a device that should be, at the same time, very compact and "portable", simple in terms of assembly and data acquisition and handling (in order to be used as a beam-diagnostics device), cost-effective and finally capable of $O(100\ \mu\text{m})$ resolution in at least one coordinate in a high-rate (up to MHz/mm^2) environment.

The main idea is very simple: to enlarge the drift gap from a few mm up to several cm, in order to deduce the coordinate along the drift direction from a precise drift-time measurement; the main limitation is coming essentially from electron diffusion (see Fig. 4).

After some GARFIELD simulation studies, we have realized a compact TPC starting from a standard 10×10 cm^2 triple-

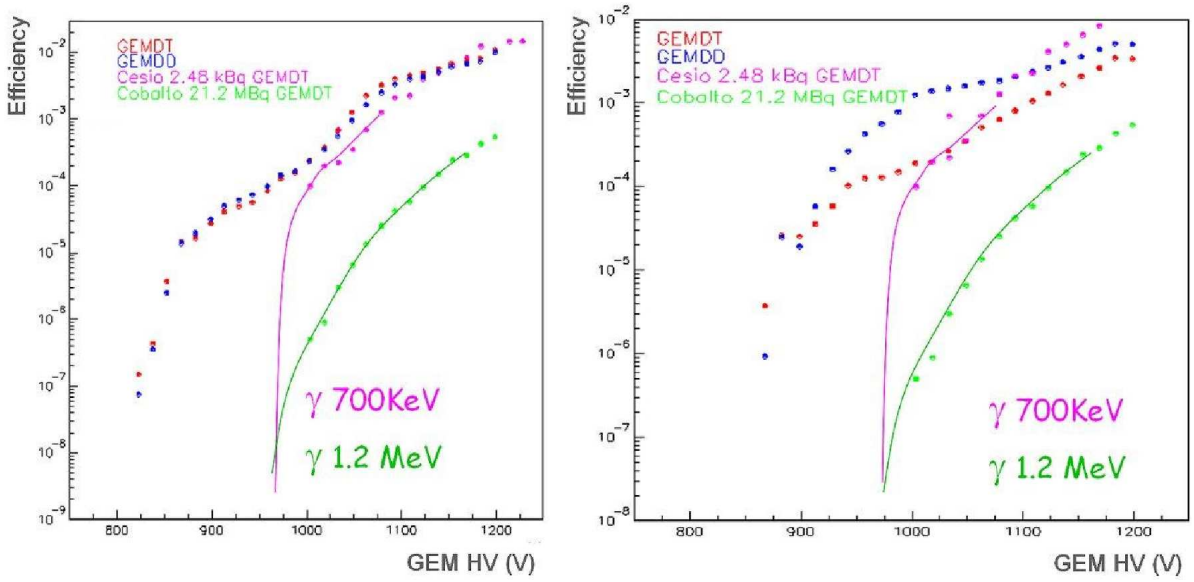

Figure 3: Neutron efficiency as a function of the total gain (overall HV) for the low-threshold detector half (DD, dark data points) and for the high-threshold part (DT, light data points): data with 14 MeV neutrons (left panel) and 2.5 MeV neutrons (right panel). The additional two sets of points and lines indicate the efficiencies to the γ-sources (0.7 MeV: upper lines, and 1.2 MeV: lower lines); a steep threshold in gain is clearly visible at about 970 V, corresponding to a gain of $\approx 10^3$.

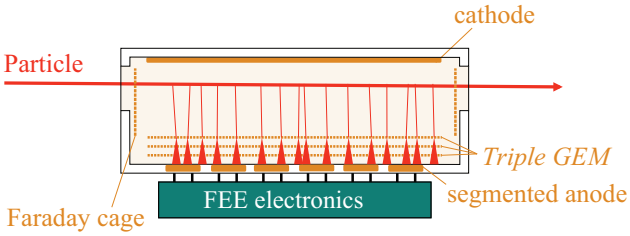

Figure 4: Compact time-projection GEM working principle.

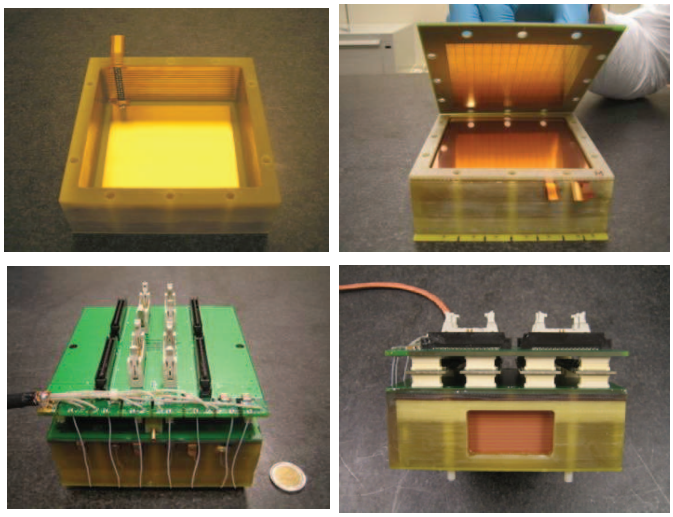

Figure 5: Assembly of the compact time-projection GEM: we use a G10 frame to create an enlarged (40 mm) drift space above the three GEM foils, with two kapton windows for the beam passage. A field-cage is also added in a following phase, in order to better define the electric field lines. The top of the "box" is closed by the anode with pads on the inner side, and on the external side the motherboard with Carioca-chip read-out cards and the HV supply.

GEM with 3/1/2/1 mm gaps and enlarging the 3 mm drift space to 40 mm through a modified G10 spacer. In order to have the smallest possible material budget we have cut two windows in the G10 spacer, for beam entrance and exit. A picture of the assembly phase clearly showing the enlarged drift space is shown in Fig. 5.

As a consequence of the much longer drift distance, the electric field lines towards the first GEM foil are deformed, so that the peripheral areas of the detector tend to have a much lower efficiency. In order to compensate this effect we have followed the following two strategies:

- Add a field-cage, all around the drift gap, in order to better shape the electrical field. The field-cage is made up by 14 copper strips, 2.5 mm wide and spaced by 5 mm, glued on both sides of kapton foils in such a way to run all around the four lateral faces of the drift gap. The strips are interconnected through 10 MΩ resistors;

- Reduce the active area of the detector to a smaller portion of the 10×10 cm^2 section. This also implies that smaller pads can be used (keeping the number of readout channels fixed at 128); in the present detector, 3×6 mm^2 pads are arranged in a 16×8 matrix, thus covering the 5×5 cm^2 central area of the anode.

In Fig. 6 the field-cage and the anode with the smaller pads are shown.

The choice of the gas mixture and electrical fields is important with respect to the achievable resolution of the TPG: we should compromise between low drift velocity, low electron diffusion, and no ageing effect. In particular, in order to fully exploit the precision of the TDC measurement of the LVDS signals coming from the Carioca-GEM chip, we have optimized

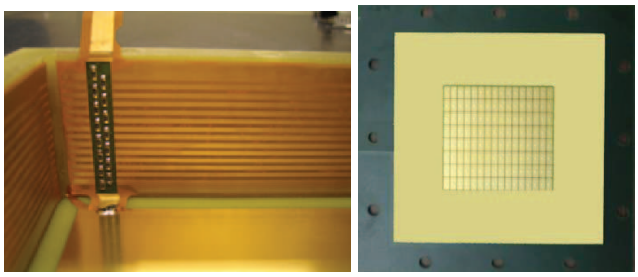

Figure 6: Left: the 14 metallized strips making up the field-cage. Right: the TPG anode segmented in 8×16 pads, 6×3 mm^2 each.

the drift field to be relatively small (at the level of 0.3 kV/cm), so that the drift velocity can be kept at very low values, while keeping the diffusion under control: for the standard Ar/CO_2 (70/30) gas mixture we have a drift velocity of $v_d = 0.5$ cm/μs and the longitudinal and transverse diffusion coefficients are at a level of $\sim 150\mu$m/$\sqrt{\text{cm}}$.

We have tested the TPG detector with electron beams at the Frascati BTF, and with a proton beam during crystal characterization measurements for the UA9 channeling experiment, at the SPS H8 beam-line. In both cases we have run the triple-GEM structure at a gain of $\sim 10^4$ and we have set the equivalent threshold on the Carioca-GEM to about 7 fC.

In the H8 setup, the TPG was placed at about 40 m from the bent crystal goniometer, so that a point resolution of 200 μm (in the z coordinate along the drift) should translate in an angular resolution of 5 μrad. In Fig. 7 a typical example of tracks measured by the TPG detector is shown: in the plots in this figure, two tracks are crossing the TPG at the same time, and can be pretty well distinguished, since we have been using a multi-hit TDC.

In order to estimate the spatial resolution, we plot in the same figure the residual of the track: $= z_{meas} - z_{inter}$. For a given pad, the measured z coordinate is given by the TDC value times the drift velocity (measured to be 0.5 cm/μs), while the interpolated z is reconstructed from the track fit from all other fired pads (except the one we are considering). Already without a correction for the different time-offsets from pad to pad, a residual of $\sim$ 200 μm is obtained.

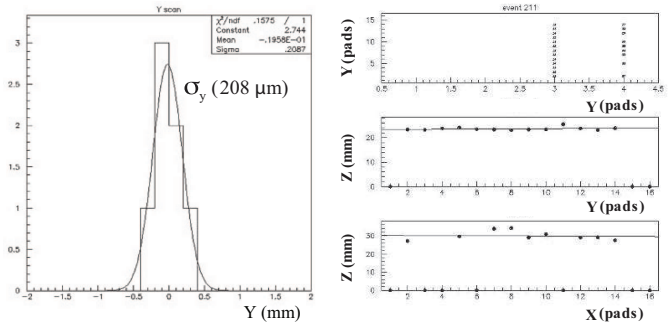

Figure 7: Right: "lateral view" of the two TPG tracks and separate "top" views of the same two tracks. Left: residuals of the track fit (residual= $z_{meas} - z_{inter}$).

The orientation of the TPG with respect to the incoming beam is shown (together with the reference system) in the schematic drawing in Fig. 8. Since the expected channeling

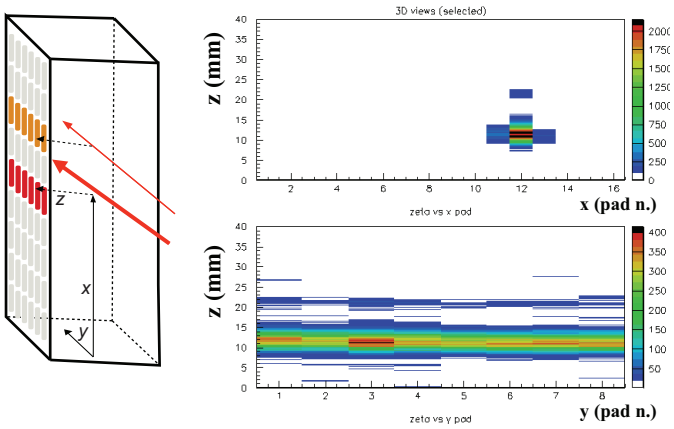

Figure 8: TPG reconstruction of channeling: "front" view (z vs. x) and "lateral" view (z vs. y) of the primary and channeled beam.

angle for the crystal under test was 270 μrad, at a distance of $\sim$ 40 m a deflection of about 11 mm was expected. In Fig. 8 indeed both the main, undeflected beam, and the portion of beam being channeled are clearly separated in the TPG data.

As a confirmation that the peak of particles at 11 mm from the main beam is due to channeled particles, we show in Fig. 9 the coordinate along the drift direction, z, as a function of time (event number) during an angular scan of the goniometer holding the crystal: the channeled beam is neatly visible only when the channeling conditions are met.

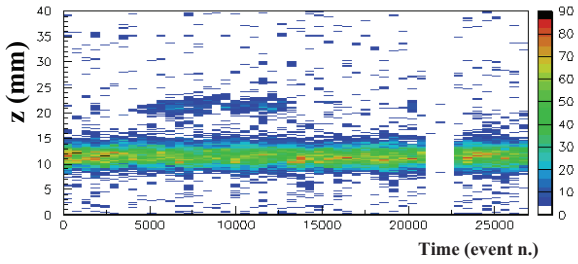

Figure 9: TPG reconstruction of the z coordinate versus time (number of event) during a crystal angular scan: the channeled beam is clearly visible at $\sim$ 10 mm from the primary beam when the channeling conditions are met .

References

[1] F. Sauli *et al.*, Nucl. Instr. and Meth. **A 386** (1997) 531.
[2] G. Bencivenni *et al.*, Nucl. Instr. and Meth. **A 488** (2002) 493.
[3] W. Bonivento, et al., Nucl. Instr. and Meth. **A 491** (2002) 233.
[4] G. Corradi *et al.*, Nucl. Instr. and Meth. **A 572** (2007) 96.
[5] W. Scandale *et al.*, CERN-ATS-2009-131 (2009).
[6] R. Villari *et al.*, Proceedings of SORMA conference (2008).